*Int. J. Heat Mass Transfer.* Vol. 34, No. 9, pp. 2237–2250, 1991
Printed in Great Britain

0017–9310/91 $3.00 + 0.00
Pergamon Press plc

# Heat transfer enhancement by electroconvection resulting from an injected space charge between parallel plates

F. M. J. McCLUSKEY† and P. ATTEN

Laboratoire d'Electrostatique et de Matériaux Diélectriques, Centre National de la Recherche Scientifique, Avenue des Martyrs, B.P. 166 X, 38042 Grenoble Cedex, France

and

A. T. PEREZ

Dept. Electronica y Electromagnetismo, Facultad de Fisica, Avenida Reina Mercedes S/N, 41012 Sevilla, Spain

(*Received* 8 *September* 1988 *and in final form* 2 *October* 1990)

**Abstract**—An examination of heat transfer between two parallel plates due to electroconvection is presented. Unipolar ion injection can be brought about at either the upper or lower electrode with heating of the liquid layer from above or below (stable or unstable stratification). The four possible configurations are treated separately. For the transitory regime, an analysis is carried out from which it is possible to calculate the thermal Nusselt number by considering an analogy between the experiment and an electric circuit of a resistance and capacitor in parallel. The values thus approximated, showing increases of up to an order of magnitude in the Nusselt number show very good agreement with the steady-state data. It is thus demonstrated that the electrical effects dominate totally over buoyancy effects for all cases considered. A short analysis of the steady state yields the relevant parameters governing the heat transfer: $Id^3$ for the fully turbulent flow and $IVd^3$ in non-turbulent conditions.

## 1. INTRODUCTION

NATURAL convection of heat in a fluid often shows itself to be a relatively inefficient means of thermal transfer with many industrial processes using mixed convection or other outside body forces to make flows more turbulent. Therefore, the idea of imposing such constraints on thermal flows has the aim of enhancing mixing and thus heat transfer within the fluid. In particular, using electrical forces to this end is referred to as electro-thermohydrodynamics (ETHD). Work on this subject dates back to the mid-1930s with Senftleben and Braun's experiments using gases [1] and then those of Ahsmann and Kronig [2] in 1950 on liquids. In the last 35 years, development of this topic has continued and today there is a large amount of published work dealing mainly with the application of the process to heat exchangers, pool boiling, condensation, fusion, etc. To discuss this literature in detail would bring us well outside the scope of this paper and we content ourselves to citing the excellent review by Jones [3] where a complete bibliography is given along with a classification of the various theoretical and experimental studies already carried out.

On a more fundamental level, we may distinguish between three different types of electrical force acting on a fluid once a voltage difference is applied across it: the Coulomb force $qE$ ($q$ is charge density; $E$ is the electric field); the dielectric force $-(E^2/2)\nabla\varepsilon$ ($\varepsilon$ is the permittivity of the fluid); and the electrostrictive force $\nabla[(E^2/2)\,(\delta\varepsilon/\delta\rho)]$ ($\rho$ is the fluid density). For the second of these, the permittivity gradient within the liquid would be induced by the imposed temperature gradients (see for example refs. [4–6]). However, under d.c. conditions with space charge creation in the fluid, this force is very weak compared to the Coulomb force. It is usual to include the electrostrictive term with the pressure. The dominant electrical body force under these conditions is then the Coulomb force $qE$. Physically, this refers to the effects of the imposed electric field on the free charge (or the space charge) present in the liquid. Generally, in experiments to date, this charge resulted from a thermally induced conductivity gradient within the liquid (see for example refs. [7–13]). Stability studies in this particular case were carried out mainly by Hoburg and Melcher [11–13] and by Takashima and Aldridge [7]. However, this type of space charge production is relevant to ohmic or quasi-ohmic liquids, where a temperature gradient will give rise to a conductivity gradient $\nabla\sigma$ ($\sigma$ is the electrical conductivity of the liquid) and the charge density $q$ is given by

$$q = -(\varepsilon/\sigma)E\cdot\nabla\sigma. \tag{1}$$

For dielectric liquids of low conductivity another

† Present address: Department of Mechanical Engineering, University of Surrey, Guildford, Surrey GU2 5XH, U.K.

## NOMENCLATURE

| | |
|---|---|
| $C_i$ | injection strength parameter, $q_i d^2/\varepsilon V$ |
| $C_p$ | specific heat |
| $d$ | electrode gap |
| $E$ | electric field |
| $g$ | gravitational acceleration vector |
| $H$ | heat flux |
| $I$ | electrical current |
| $j$ | current density |
| $K$ | ion mobility |
| $m$ | mass |
| $M$ | mobility parameter, $(\varepsilon/\rho)^{1/2}/K$ |
| $Ne$ | electrical Nusselt number |
| $Nu$ | Nusselt number (see also equation (22)), $Hd/\kappa\Delta T$ |
| $Pr$ | Prandtl number, $\nu/\chi$ |
| $q$ | charge density |
| $Q$ | total heat furnished to cell |
| $Ra$ | Rayleigh number, $\beta g \Delta T d^3/\chi\nu$ |
| $Re$ | Reynolds number, $w'd/\nu$ |
| $S$ | surface area |
| $t$ | time |
| $T$ | temperature |
| $T'$ | stability parameter (see equation (2)), $\varepsilon V/K\eta$ |
| $\Delta T$ | temperature difference between electrode plates |
| $V$ | applied electrical voltage |
| $w$ | velocity component perpendicular to electrode. |

Greek symbols

| | |
|---|---|
| $\beta$ | thermal expansion coefficient |
| $\varepsilon$ | liquid permittivity |
| $\eta$ | dynamic viscosity of liquid |
| $\theta$ | temperature fluctuation |
| $\kappa$ | thermal conductivity |
| $\nu$ | kinematic viscosity of liquid |
| $\rho$ | density of liquid |
| $\sigma$ | electrical conductivity |
| $\tau$ | time constant |
| $\chi$ | thermal diffusivity |
| $\Omega$ | control volume. |

source of free charge becomes dominant compared to this. This second process of charge creation is referred to as ion injection, and occurs at one or both electrodes. It is a common phenomenon, taking place whenever an electric field is applied between two metal electrodes in an insulating liquid [14]. Our experiments to date indicate that, to first approximation, this charge injection, and hence the Coulomb force, may be considered as being independent of temperature gradients. Little other work has been done on this particular case of electroconvective heat transfer in liquids brought about by space charge injection at an electrode. In gases, however, Franke [15] among others showed an increase in heat transfer in air using the ionic wind brought about by corona injection. A theoretical analysis as well as some experiments were carried out by Lazarenko *et al.* [10], who also derived some relevant non-dimensional parameters. Some preliminary experiments were performed with forced flows in tubes using radial fields by Fernandez and Poulter [16]. A more thorough analysis on this has recently been presented by Mizushina *et al.* [17] with some interesting results. Stability analysis of the electroaerodynamic case was carried out by Hoburg [18] who also demonstrated experimentally the increase in Nusselt number due to injection [19]. Finally, before presenting our work here, let us make note of the paper by Bologa *et al.* [20] who examined the heat transfer augmentation due to an electric field being imposed across a gas–solid suspension flow. They examined the cases for both conducting and insulating particles. We mention this since under certain conditions, flow structures due to the motion of dielectric charged particles in air are quite similar to those due to ions in dielectric liquids [21].

The problem we are examining here is that of attempting to characterize the heat transfer augmentation in a simple geometry of a horizontal liquid layer between two parallel plates subject to a temperature gradient and an electric field. Depending on the sign of the latter, ion injection may be induced on the upper or lower plate electrode. Two further cases are considered when we change from unstable to stable thermal stratifications. We carried out all experiments at fixed heat flux.

In the next section we give a résumé of what is known of electrohydrodynamic (EHD) flows in dielectric liquids due to unipolar ion injection and attempt to give an intuitive idea of this phenomenon since it is unlikely that researchers in pure heat transfer will be familiar to any great extent with EHD. We will also briefly mention the classical Rayleigh–Bénard problem before presenting our experimental set-up. Thereafter the experimental results in both transient and steady-state regimes are presented and discussed in the light of some mathematical modelling of the phenomena.

## 2. ELECTROCONVECTION AND NATURAL CONVECTION

When a layer of insulating dielectric liquid, confined between two plane parallel metallic electrodes, is subjected to an applied d.c. voltage $V$, the current passing through the circuit will generally have a variation

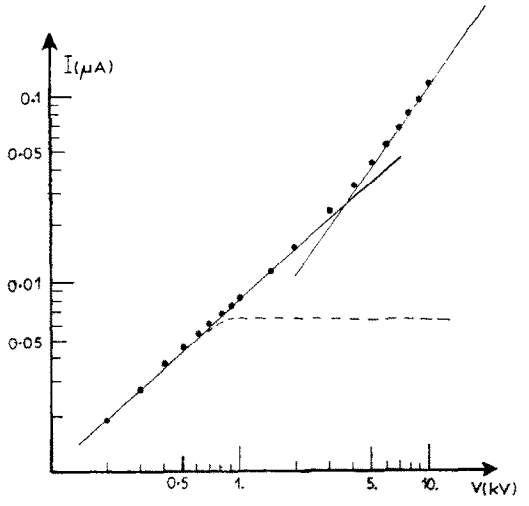


FIG. 1. Typical current voltage characteristic for silicone oil plus TiAP in the experimental cell. The dashed line indicates the theoretical saturation current.

similar to that shown in Fig. 1. Clearly there are two different electrical conduction regimes. For low voltages (the ohmic regime), the current $I$ varies proportionally to $V$ and is due to a slight perturbation by the electric field of the equilibrium between the dissociation of electrolytic impurities and recombination of ions in the liquid bulk. The dissociation process is limited and therefore the current, in theory, will eventually saturate. However, this does not happen and for higher voltages, $I$ increases and varies as $V^{\alpha}$ with $\alpha > 1$. Félici [14] demonstrated that this is due to a second source of charge at (at least) one of the electrodes, an unavoidable phenomenon when using metal electrodes in liquids. This is ion injection and it is electrochemical in nature [14, 22]. Usually we deal with injection at one electrode only. This was verified by electro-optic measurements of the electric field which showed it to be lower on one electrode (injector) and higher on the other (collector). In such cases we refer to unipolar ion injection. The variation of the current with the voltage depends on the injection strength and on movement of the liquid. Such motion was clearly pointed out via Schlieren techniques [23, 24]. (Note that the typical currents involved are particularly low—in our apparatus $I$ is of the order of a microampere—and magnetic effects are totally negligible.)

The problem of hydrodynamic stability of a layer of insulating liquid subjected to unipolar ion injection has been well analysed [25, 26]. Briefly, the electric field increases as we move away from the electrode where injection occurs. From the current density relationship: $j = qKE$ ($=$ constant) ($K$ is ionic mobility), the charge density $q$ must be decreasing away from the injector. This is a potentially unstable situation. (This is similar to the Rayleigh–Bénard problem of a horizontal fluid layer heated from below. In that case, the temperature is a decreasing function with height while liquid density increases.) Intuitively, if we consider the virtual displacement of a fluid 'parcel' which conserves its charge towards the collector, we see that it is then subject to a greater Coulomb force (buoyancy force for the Rayleigh–Bénard case) than the fluid immediate to it. It will thus have a tendency to continue its displacement towards the collector. The coupling between charge and velocity perturbations is then positive [27].

However, instability as a result of this positive coupling will only occur if the electrical (buoyancy) force is strong enough to overcome viscous damping [28, 29] ([30]). The ratio between the electrical and viscous forces is the stability parameter $T'$ [26] given by

$$T' = \frac{\varepsilon V}{K\eta} \tag{2}$$

where $\eta$ is the dynamic viscosity of the liquid. (In the Rayleigh–Bénard case the relevant stability parameter is the Rayleigh number [31].) Perturbations of small amplitude are damped out for $T'$ less than some critical value, say $T_c$, and amplified for higher values. The numerical value of $T_c$ depends on the non-dimensional injection strength parameter $C_i$

$$C_i = q_i d^2/\varepsilon V. \tag{3}$$

Here $q_i$ is the injected space charge density at the injector and $d$ the electrode gap. See also Appendix A for an explanation and evaluation.

Though there are a number of similarities between this and the Rayleigh–Bénard problem, there is a rather fundamental difference also. In the EHD case, the ions also move relative to the liquid with a 'drift velocity' $KE$. The importance of this ionic drift was brought into the open in a non-linear stability analysis by Atten and Lacroix [32]. They demonstrated the existence of a finite amplitude solution to the governing equations for subcritical conditions. That is, there exists for $T' < T_c$ (linear stability criterion), a non-linear stability criterion $T_f$, such that, for $T_f < T' < T_c$, there is a stable solution with maximum velocity amplitude greater than the drift velocity. This indicates the presence of hysteresis phenomena for both velocity and current, a situation which was confirmed experimentally [28, 32]. (This does not arise for Rayleigh–Bénard convection.)

Above the critical stability value, the liquid motion has an important effect on charge transport in the case of strong unipolar injection. When $T' < T_c$, the ions cross the electrode gap with velocity $KE$. For $T' > T_c$, two major regimes of motion are characterized: a viscous regime where the Reynolds number $Re$, evaluated with the maximum velocity amplitude is much less than 10, and an inertial regime where it is much greater than 10. In other words, for $Re \ll 10$ the movement is structured such that the horizontal scale of the largest convective cells is of the same order of

magnitude as the electrode gap (cf. cellular Rayleigh–Bénard convection). A semi-quantitative analysis shows the vertical velocity $w'$ to be proportional to $V^2$ and the current $I$ to $V^{5/2}$ [28, 29]. An electrical Nusselt number $Ne$ was defined for the current (analogous to that used in thermoconvection) and this was found to vary as $(T'/T_c)^{1/2}$.

For $T' \gg T_c$, the movement becomes fully turbulent ($Re \gg 10$). Charge density perturbations are very small compared to the mean value (nonpermanence of any cellular structure) and $w'$ varies linearly with $E$ [29]. Félici [33], by considering the conversion of electrical energy ($\frac{1}{2}\varepsilon E^2$) to mechanical energy ($\frac{1}{2}\rho w'^2$) developed the concept of an electrohydrodynamic mobility $(\varepsilon/\rho)^{1/2}$. Experimental measurements showed that $w' \approx \frac{1}{3}(\varepsilon/\rho)^{1/2}E$ [28, 29]. The ratio between the EHD mobility and the true ion mobility $K$ is the parameter $M\,(=(\varepsilon/\rho)^{1/2}/K)$. The current $I$ in this regime varies as $V^2$ and $Ne$ is constant $(=\sqrt{(M/3)})$.

To finish, we refer readers to a number of interesting articles and references therein on Rayleigh–Bénard convection [34–41]. Few analytical attempts to account for the experimental observations have been tried, the most noteworthy being that of Kraichnan [42].

## 3. EXPERIMENTAL SET-UP AND PROCEDURES

### 3.1. *The experiment*

The liquid layer was confined between two copper plate electrodes (active surface area $15.75 \times 10.4$ cm$^2$) and a side wall unit of Plexiglas. The electrode gap $d$ could be changed by replacing the Plexiglas frame ($d = 3$, 5 or 7 mm). One of the electrodes, which we will call plate 2, was kept at constant temperature via the circulation of silicon oil† inside it from a thermostated bath. This plate was covered in polyurethane foam to avoid any heat loss to or gain from the surroundings. The other electrode (plate 1), of mass 2.48 kg had a heating resistance attached to it which could furnish between 0 and 30 W of power. We operated at constant heat flux. The entire apparatus was placed inside a thermally insulated box which could be 'turned over' in order to have the heat flux from the bottom or from the top of the fluid layer (see Fig. 2).

The temperatures of the plates were measured using platinum probes and a high precision thermometer ($\pm 0.01$°C). One probe was placed in direct contact with plate 1. However, since the high voltage (positive or negative) was applied to plate 2, there was some difficulty in measuring its exact temperature. It was necessary to electrically insulate the probe, while at the same time ensure as good a thermal contact as possible. We got around this problem by attaching the probe to the end of a small sapphire rod, the other end of which was covered in a thin layer of silver and soldered to the copper plate. (Sapphire is an excellent heat conductor and a good electrical insulator.) To minimize thermal losses around this probe, we surrounded the sapphire rod with two copper bells, both soldered to the plate electrode (see Fig. 2). The whole was then covered in a thick layer of polyurethane. Electrical connections from the probe to the thermometer were made via an araldite tube which crossed through the polyurethane and insulated them from the high voltage. To protect the probe from possible electrical breakdown between it and the nearest copper bell, a small metal sphere was placed around the probe at the top of the sapphire rod and earthed (Fig. 2).

The outer container was made of wood, polyurethane and aluminium and was thermostated using a second bath. The temperature inside the container was kept equal to that of plate 1, so that this plate would lose no heat to the surroundings. Therefore, the heat furnished to plate 1 via the heating resistance passed entirely through the cell.

The probe on plate 2 was calibrated using a third probe attached to the active surface of that plate. This was carried out at zero applied voltage. Thus, via the calibration, we could measure instantaneously the temperatures on each plate ($T_1$ and $T_2$) as well as the temperature difference $\Delta T$ across the layer. The overall error in the measurements was never greater than 3% for all the results reported here (for $\Delta T > 1$°C, the error does not exceed 2%, the precision for $\Delta T$ being $10^{-2}$°C). In the experiments we recorded both steady-state values and the evolution in time of $\Delta T$ until steady state.

The working liquid was silicone oil (Rhodorsil 47 V 10), with relative permittivity $\varepsilon_r = 2.63$; density $\rho = 9.3 \times 10^2$ kg m$^{-3}$; kinematic viscosity $\nu = 10^{-5}$ m$^2$ s$^{-1}$; specific heat $C_p = 1.63 \times 10^3$ J kg$^{-1}$ C$^{-1}$ and thermal conductivity $\kappa = 0.13$ J m$^{-1}$ C$^{-1}$ s$^{-1}$. The liquid was saturated with the salt TiAP [22, 43] in order to provoke a steady ion injection at one of the electrodes. For copper electrodes with silicone oil and TiAP we verified that there is an injection of negative charge from the cathode. Thus, positive voltage applied to plate 2 results in negative charge injection from plate 1, whereas negative voltage causes it to occur from plate 2.

Thus, by turning the cell 'upside down' or not and by changing the polarity (or sign) of the applied voltage we have four possible situations: (i) heating and injection from below or (ii) from above, (iii) heating from below and injection from above or (iv) heating from above and injection from below. Results were obtained for each case. Theoretical analysis of the stability of each of these situations shows the importance of distinguishing between them at least around the critical values of $T'$ and $Ra$ [44].

Before presenting the results for combined ion injection and temperature difference we will first give the

† With this electrode brought into contact with the high voltage source, the cooling liquid had to be electrically insulating in order to avoid any electrical leakage.

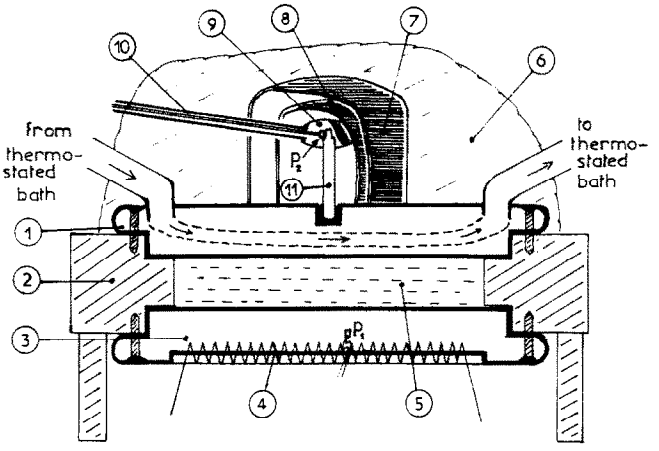


FIG. 2. Schematic of the experimental cell: 1, fixed temperature copper plate; 2, Plexiglas frame; 3, heated copper plate; 4, heating resistance; 5, liquid layer; 6, polyurethane layer (thermal insulation); 7, outer copper dome; 8, inner copper dome; 9, earthed copper protection around probe $P_2$; 10, araldite tube containing connections from probe $P_2$; 11, sapphire rod. $P_1$ and $P_2$ are the temperature probes (platinum).

electrical characteristics of the cell and a rundown of the method of evaluation of the thermal Nusselt number $Nu$, which characterizes the non-dimensional heat transfer across the layer.

### 3.2. *Isothermal electrical results*

Figure 1 shows a typical current voltage curve taken between two experimental runs. The injection current varies as $V^{\alpha}$ with $\alpha \approx 1.5$ for $V \geqslant 4$ kV. We must separate the two components of the current: the conductive (ohmic) one and the injection one, since only the latter is relevant in the Coulomb force term $qE$. This is done by evaluating the saturation level of the former and subtracting it from the total current (dashed line indicates the saturation current). The corresponding saturation voltage (that for which the current begins to saturate) in the example in question is about 750 V.

To evaluate the non-dimensional injection parameter $C_i$, we make use of appropriate curves given by Denat [45] (see also Appendix A). In most of our experiments $C_i$ varied from about 0.55 ($V = 3$ kV) to 0.15 ($V = 15$ kV). These values are not very high and indicate that charge injection is rather weak. Under such circumstances, we may roughly consider that the harmonic uniform electric field is not dramatically perturbed by the presence of the injected space charge.

### 3.3. *Heat flux evaluation (steady state)*

The heat flux across a fluid medium contains a contribution from conduction and from convection processes if the fluid is in motion. It is usually written in the form

$$H = -\kappa \nabla T + \rho C_p w' T \tag{4}$$

($w'$ is the velocity component normal to the plates). The global effect of convective heat transfer is written in terms of the Nusselt number $Nu$, which is the ratio of the mean heat flux $\bar{H}$ to the flux $\bar{H}_0$ which would exist without convection for the same temperature difference

$$Nu = \frac{\bar{H}}{\bar{H}_0} = \frac{\bar{H}}{-\kappa \Delta T/d} = \frac{|\bar{H}|\, d}{\kappa \Delta T}. \tag{5}$$

Nusselt number $Nu$ is normally plotted as a function of the Rayleigh number $Ra$ (proportional to the temperature difference)

$$Ra = \frac{\beta g \Delta T d^3}{\chi \nu} \tag{6}$$

where $\beta$ is the coefficient of thermal expansion of the liquid and $g$ the gravitational acceleration. To evaluate $Nu$, we assumed the heat flux could be written in the form

$$\bar{H} = \frac{-\kappa_{app} \Delta T}{d} \tag{7}$$

where $\kappa_{app}$ is an effective or apparent heat conductivity. This gives

$$Nu = \frac{\kappa_{app}}{\kappa} \tag{8}$$

leaving us to determine $\kappa_{app}$ for the liquid only. In our experiment, the total heat $Q$ breaks into two components: one across the liquid ($H_L$) and the other across the Plexiglas ($H_P$)

$$Q = S_L H_L + S_P H_P \tag{9}$$

($S_L$ and $S_P$ are the surface areas of the copper plate–liquid, and the copper plate–Plexiglas interfaces, respectively). Using equation (7) this may be written as

$$Q = \frac{S_L \kappa_{app} \Delta T}{d} + \frac{a S_P \kappa_P \Delta T}{d}. \tag{10}$$

The constant '$a$' is included to account for the geometrical shape of the Plexiglas frame as well as for

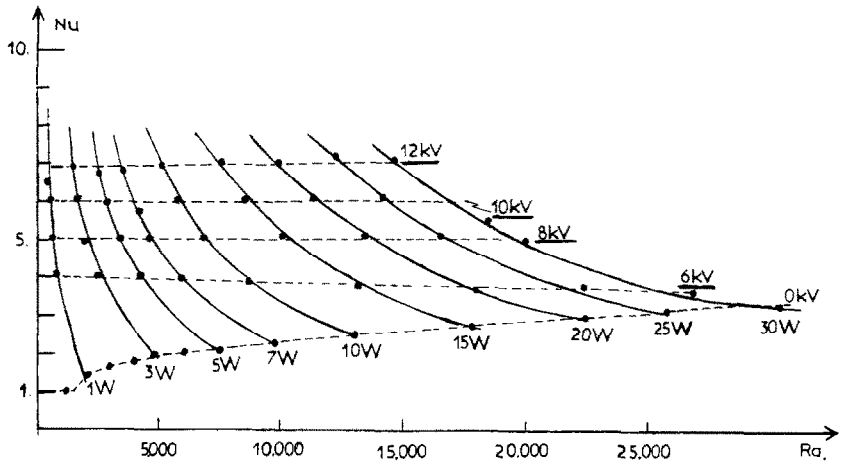


FIG. 3. A full set of results for an inter-electrode distance of 5 mm, for different applied voltages and heat fluxes, with heating and injection from below, as a function of $Ra$.

any lack of thermal contact between it and the copper plates. Its value was determined experimentally under purely conductive conditions and we found $a \cong 0.27$.

The value of $Nu$ as a function of $Ra$ (for no applied electric field) is shown on Fig. 3 (lowest curve) and agrees very well with the already known results (see for example ref. [46]). The good agreement between our experimental results and the classical ones constitutes a test for our experimental set-up.

## 4. EXPERIMENTAL RESULTS

### 4.1. *Steady-state results*

Results obtained when heating and injection both occurred at the lower electrode are given on Fig. 3 for $d = 5$ mm. Values were obtained by either fixing the heat flux and varying the applied voltage, or, fixing the voltage (and to first approximation the injection strength) while varying the heat flux to the liquid ($H$). In the former case for each given heat flux ($H$) the experimental points lie on a hyperbolic curve (full lines). This is because of the definition of $Nu$ (see equation (5)) which is effectively proportional to $1/\Delta T$, that is, to the inverse of the Rayleigh number. Then, when we increase $V$, and thus the Coulomb force, the agitation of the liquid also augments. This causes convective transport to be greater. The temperature difference between the plates will then drop and consequently $Nu$ will rise.

When working at fixed, high enough $V$ and variable $H$, we see that $Nu$ is, to first approximation, constant. It does not appear to depend on the Rayleigh number at least within the range of voltages ($V \geqslant 6$ kV) and heat fluxes we used. We conclude that the convective transfer of heat is essentially determined by the electrical forces, with buoyancy forces remaining globally unimportant. This conclusion was confirmed by the lack of any significant sensitivity of $Nu$ on the configuration used (heating or injecting independently

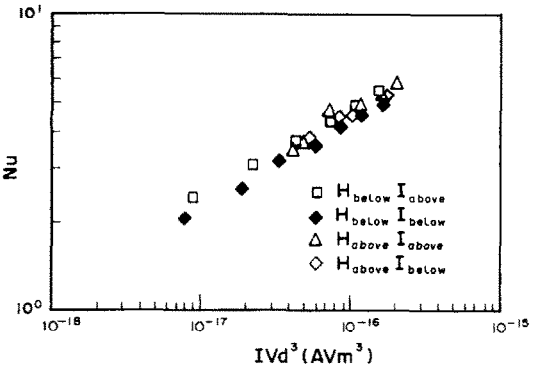


FIG. 4. $Nu$ as a function of $IVd^3$ for $d = 3$ mm with heating and injection independently from above and below.

from above or below), as we can see from the experimental points on Fig. 4. The values of $Nu$ are plotted as a function of $I_{inj}Vd^3$, since we estimate the flow here to have a Reynolds number of about 10 (approximately viscous dominated motion). A justification of this choice of parameter is given in the short analysis of Section 5. For the ensemble of the results (different configurations and three liquid layer depths), it is interesting to check for some type of asymptotic behaviour for $Nu$. The set of Nusselt numbers gained from our experiments are too weak for a proper examination of this, though we can get some insight on the convective transport by looking at the variation of $(Nu-1)$. Effectively $Nu$ takes the form [47]

$$Nu = 1 + \langle q^* w^* \rangle \tag{11}$$

where $\langle q^* w^* \rangle$ is a non-dimensional term representing the advective transport of heat. Clearly, plotting $(Nu-1)$ against the electrical parameter gives an indication of the behavioural tendencies of the convection only. This case differs from classical Rayleigh–Bénard

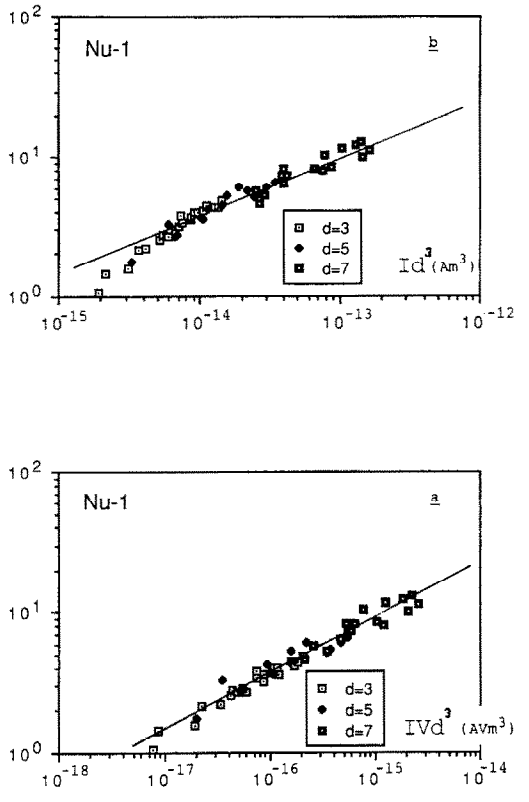


FIG. 5. $(Nu-1)$ as a function of (a) $IVd^3$ and (b) $Id^3$. The best fit for (a) is $(IVd_3)^{0.36}$ and for (b) is $(Id^3)^{0.43}$.

convection, in that here, the velocity field depends almost exclusively on electrical forces (in the following we consider temperature as a passive contaminant transported by a forced advective motion induced by the Coulomb force).

Figure 5 shows $(Nu-1)$ as a function of both $I_{inj}Vd^3$ (viscous regime) and $I_{inj}d^3$ (inertial regime). Both are presented since we can only estimate an order of magnitude of the value of the Reynolds number of the motion and this is close to the transition value between regimes. In Fig. 5(a) $(Nu-1)$ varies as $(I_{inj}Vd^3)^n$, where $n \cong 0.36$ and in Fig. 5(b) as $(I_{inj}d^3)^m$ where $m \cong 0.43$. Both of these numbers were obtained via a least squares fit. The dispersion of the points is rather small. (From here on we will write $I_{inj}$ as $I$.)

Clearly, from these curves, with the experimental results seeming to fit some power law for either parameter we are left with the rather unenviable task of deciding which is most relevant. The chief difficulty here lies with the fact that we cannot measure the velocity and thus evaluate the Reynolds number. We can however attempt to approximate it by using a velocity expression given by Félici [48] for low injection, high voltage flows. He gave

$$w' \sim \sqrt{C_i}\sqrt{(\varepsilon/\rho)}\,E.$$

If we take a proportionality constant of approximately $\frac{1}{3}$, a typical value of the Reynolds number will be given by the expression

$$Re = \frac{w'd}{\nu} = \frac{1}{3}\sqrt{C_i}\sqrt{(\varepsilon/\rho)}\,\frac{V}{\nu}.$$

For relevant values of $C_i$ and $V$ measured throughout our experiments we find a variation for $Re$ ranging from about 10 to 30. This indicates that we are in the transition region between viscous-dominated and inertially-dominated flows.

### 4.2. *Transitory regime results*

Since, for a given voltage, the apparent thermal conductivity is more or less independent of the temperature difference, then so too, to first approximation, are the convective transport and the agitation of the liquid. This behaviour should also be found in the transitory evolution of the system. For example, if we consider a weak perturbation of a given steady state (modification of applied voltage or of heat supplied to the bottom plate) it is possible to make an analogy with an electrical circuit. If we change the voltage, then the effective thermal conductivity (electrical conductance) is rapidly altered, the characteristic time being that of ion transit between electrodes. Alternatively, if we change the heat flux (i.e. the current in an electrical circuit), the effective thermal conductivity (electrical conductance) remains unchanged. In both cases, relaxation to a new steady state will occur via the cooling or heating of the bottom plate (which plays the role of a capacitor). Thus we have the equivalent of a circuit of a resistance and a capacitor in parallel and we expect the relaxation to be exponential in time.

This is effectively what we see when we fix $V$ and vary the heat flux by small increments between steady states (Fig. 6). Each change in heat flux leads to the same characteristic time. From the results we should be able to determine the 'conductance' and evaluate $\kappa_{app}$ and $Nu$. A mathematical expression can be developed for this and its derivation is given in detail in Appendix B. Basically, we use the heat conduction equation

$$\rho C_p \frac{\delta T}{\delta t} + \nabla \cdot H = 0 \tag{12}$$

integrated over the different media (copper and silicone oil) and solve the final first-order ordinary differential equation to obtain the following expression for the temperature difference between the two plates as a function of time assuming no liquid motion. (The nomenclature is also explained in the appendix.)

$$T_1(t) - T_2 = (T_1(0) - T_2)\exp\left(\frac{-t}{\tau}\right) + \frac{Q(d_2 - d_1)}{(S_L\kappa_L + aS_p\kappa_p)}\left(1 - \exp\left(\frac{-t}{\tau}\right)\right) \tag{13}$$

where $Q = S_C H_0$ is the heat supplied and

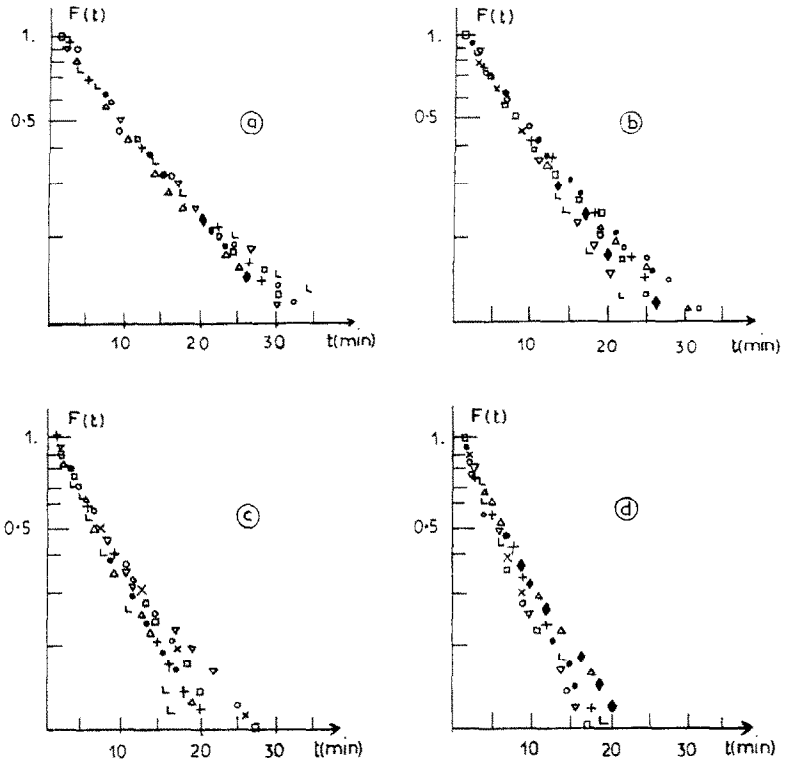


FIG. 6. The function $F(t) = (T_1(t) - T_1(\infty))/(T_1(0) - T_1(\infty))$ as a function of time. (a) $V = 6$ kV; (b) $V = 8$ kV; (c) $V = 10$ kV; (d) $V = 12$ kV. +, 1 W; ●, 3 W; △, 5 W; □, 7 W; ○, 10 W; ×, 15 W; ▽, 20 W; ◆, 25 W; L, 30 W.

$$\tau = (\tfrac{1}{2}m_L C_{pL} + \tfrac{1}{2}m_P C_{pP} + m_C C_{pC}) \frac{(d_2 - d_1)}{(S_L \kappa_L + a S_P \kappa_P)}. \tag{14}$$

From equation (13) we can see that as $t \to \infty$

$$\frac{Q(d_2 - d_1)}{(S_L \kappa_L + a S_P \kappa_P)} = T_1(\infty) - T_2 \tag{15}$$

and equation (13) is then written as

$$(T_1(t) - T_2) = (T_1(\infty) - T_2) - [(T_1(\infty) - T_2) - (T_1(0) - T_2)] \exp\left(\frac{-t}{\tau}\right) \tag{16}$$

whence the exponential behaviour is seen from the function

$$F(t) = \frac{T_1(t) - T_1(\infty)}{T_1(0) - T_1(\infty)}. \tag{17}$$

In equation (14), the terms of the numerator represent the calorific capacities of the liquid, the Plexiglas and the copper, respectively, while the terms of the denominator are 'thermal conductances'.

If we replace $\kappa_L$ by $\kappa_{app}$ in equation (14), we can deduce a value for this latter by using the measured experimental value of $\tau$ taken from the curves of Fig. 6. The Nusselt numbers gained in this way are compared with the steady-state values in Table 1. Agreement is quite good which supports the validity of our assumption that the movement is controlled essentially by forced convective transfer of heat.

## 5. CRUDE ANALYSIS FOR STEADY-STATE FLOW

An analysis of electroconvective motion in isothermal conditions for space charge limited injection (i.e. very large $C_i$) has already been carried out by Lacroix *et al.* [29]. However, in our case of low to medium values of $C_i$, these results do not apply. Due to the complexity of the theoretical problem and also of the exploitation of the experimental results, we will content ourselves here with the derivation of the relevant parameters and an estimate of the power laws governing the observed phenomena. For such an analysis we make the assumption that due to the low values of $C_i$, the distortion of the electric field $E$ is weak (of the order of $C_i$) and thus may be neglected (we may write $E = V/d$). The current will also be taken to be constant for any given value of the voltage. Two regimes of motion are to be considered: the viscous dominated one for $Re < 10$ and the inertially dominated (or fully turbulent) one for $Re > 10$. Both cases must be considered since we did not have access

Table 1. The Nusselt number as a function of heat flux $Q$ (W) and of applied voltage $V$ (kV): (I) steady-state conditions; (II) time-dependent regime, using the $\Delta T(t)$ curves and equation (14)

| $V$(kV) | | $Q$(W) 1 | 3 | 5 | 7 | 10 | 15 | 20 | 25 | 30 |
|---|---|---|---|---|---|---|---|---|---|---|
| 12 | (I) | 6.82 | 7.33 | 7.12 | 7.12 | 7.23 | 7.33 | 7.33 | 7.50 | 7.40 |
| | (II) | 6.98 | 7.03 | 6.58 | 7.59 | 7.38 | 7.22 | 7.08 | 6.97 | 6.26 |
| 10 | (I) | 6.44 | 6.44 | 6.23 | 6.00 | 6.33 | 6.40 | 6.37 | 6.42 | 5.84 |
| | (II) | 6.26 | 5.89 | 5.82 | 5.25 | 5.41 | 5.34 | 6.54 | 6.10 | 7.40 |
| 8 | (I) | 5.38 | 5.25 | 5.25 | 5.30 | 5.31 | 5.39 | 5.40 | 5.40 | 5.39 |
| | (II) | 4.43 | 4.63 | 5.01 | 5.23 | 5.35 | 4.86 | 5.13 | 5.35 | 5.96 |
| 6 | (I) | 4.43 | 4.32 | 4.30 | 4.26 | 4.14 | 4.10 | 3.99 | 4.02 | 3.99 |
| | (II) | 4.35 | 3.95 | 4.10 | 3.82 | 3.83 | 3.72 | 3.64 | 3.76 | 3.71 |

to measurements of velocity during the experiments and therefore cannot fix with any certainty the Reynolds numbers. We also consider that the motion and therefore the heat transfer are controlled solely by the electrical forces.

5.1. *Velocity dependence on different parameters*

5.1.1. *Viscous dominated regime.* Here, we use the energy balance argument that energy dissipation will vary with the electrical energy density furnished by the Coulomb force (i.e. taking only the viscous terms and the body force in the Navier–Stokes equation)

$$\frac{\eta w'}{d^2} w' \sim (qE)w'. \tag{18}$$

The expression $qw'$ can be related to the current density $j = q(KE + w')$ and using the experimental fact that outside the boundary layer on the electrode, i.e. in the bulk, the velocity $w'$ is far greater than the drift velocity (see, for example refs. [23–26]) we may write

$$\frac{\eta w'^2}{d^2} \sim \frac{Vj}{d}. \tag{19}$$

We arrive at the following expression for the velocity dependence in the viscous regime of motion:

$$w' \sim \sqrt{\left(\frac{jVd}{\eta}\right)}. \tag{20}$$

5.1.2. *Inertially dominated regime.* In this case of fully turbulent flow we equate turbulent kinetic energy to the work done by the electrical force (i.e. balancing the inertial terms of the Navier–Stokes equation with the body force and integrating)

$$\tfrac{1}{2}\rho w'^2 \sim \tfrac{1}{2}qEd = \tfrac{1}{2}qV. \tag{21}$$

If we make an analogy to the Rayleigh–Bénard case, we may consider that 'blobs' of charged liquid burst from the boundary layer on the injector and move across the layer to the collector. The charge density in these blobs will keep a value $q$ very close to that at the injecting electrode $q_0$, if Coulombian repulsion is negligible, leaving us with the relation $\rho w'^2 \sim q_0 V$. The charge density $q_0$ is related to the current density $j$ via its value on that electrode

$$j = Kq_0E \cong \frac{Kq_0V}{d}. \tag{22}$$

The energy balance is then

$$\rho w'^2 \sim \frac{dj}{K} \tag{23}$$

giving the velocity dependence as

$$w' \sim \sqrt{\left(\frac{jd}{K\rho}\right)}. \tag{24}$$

5.2. *Nusselt number dependence on velocity*

The Nusselt number is defined as the observed heat flux divided by the heat flux that would occur at the same temperature difference without convective flow: i.e.

$$Nu = \frac{\kappa \nabla T + \rho C_p \langle w\theta \rangle}{\kappa(\Delta T/d)} \tag{25}$$

or upon integrating

$$Nu = 1 + \chi^{-1} \int_0^d \frac{\langle w\theta \rangle}{\Delta T} \mathrm{d}z \approx 1 + \chi^{-1} \frac{\langle w\theta \rangle d}{\Delta T}. \tag{26}$$

In non-dimensional terms, this is equivalent to saying that $Nu$ depends on the Reynolds number ($\propto w'$) and the Prandtl number ($\propto \chi^{-1}$).

5.2.1. *Viscous dominated regime.* Using the velocity expression given previously, we may therefore write

$$Nu = f_{1V}(Re) \cdot f_{2V}(Pr) = f_{1V}\left(\sqrt{\left(\frac{jVd^3}{\eta\nu^2}\right)}\right) \cdot f_{2V}(Pr) \tag{27}$$

whence we extract the relevant parameter $IVd^3$ ($\propto jVd^3$) used in Fig. 5. We may suppose, as results seem to indicate, that the function $f_{1V}$ can be approximated by a power law.

5.2.2. *Inertially dominated regime.* Using relation (26) for inertial flow the Nusselt number dependence is

$$Nu = f_{1I}(Re) \cdot f_{2I}(Pr) = f_{1I}\left(\sqrt{\left(\frac{jd^3}{K\rho\nu^2}\right)}\right) \cdot f_{2I}(Pr). \tag{28}$$

The relevant parameter in this inertial regime is seen to be $Id^3$ ($\propto jd^3$). We consider the function $f_{II}$ to be well represented also by a power law. The maximum value possible for this power law is found via the following considerations. For strongly convective flows, the Nusselt number may be approximated from equation (26) by

$$Nu \approx \frac{\chi}{\Delta T}\,{}^{1}\langle w\theta\rangle d. \tag{29}$$

Supposing that the velocity–temperature fluctuation correlation $\langle w\theta\rangle$ is very high, with the r.m.s. temperature value being proportional to $\Delta T/2$, we find that with

$$Nu \propto Re\,Pr \tag{30}$$

we get

$$Nu \sim \sqrt{\left(\frac{Id^3}{K\rho\nu^2}\right)Pr}$$

or

$$Nu \sim \sqrt{(Id^3)}. \tag{31}$$

Without a full analysis particular to the electroconvective problem, we cannot give any theoretical power law exponent in either viscous- or inertially-dominated regimes. The law given in expression (31) merely represents a maximum value of the exponent. Nevertheless, we may, for comparative purposes, attempt to deduce power laws by using results already known for the Rayleigh–Bénard case and transposing them to the ETHD one.

For viscous motion, we may refer to an order of magnitude analysis on Rayleigh–Bénard convection by Kraichnan [42], wherein for high $Pr$ fluids he showed that $Nu \propto Ra^{1/3}$, with $w'$ ($\propto Re$) $\sim Ra^{2/3}$. It is easy to deduce the relationship $Nu \propto Re^{1/2}$, which when used in expression (24) gives

$$Nu \sim (IVd^3)^{1/4}.$$

For inertially dominated flow, Chu and Goldstein [34] found experimentally that $Nu \sim Ra^{0.278}$. Deardorff and Willis [35] gave that $w'$ ($\propto Re$) $\sim Ra^{1/2}$ in this fully turbulent regime and thus we have the variation, using equation (28)

$$Nu \sim (Id^3)^{0.28}.$$

More recent experimental and analytical results [49] in the fully turbulent regime indicate that the Nusselt number varies as $Ra^{2/7}$ and that the velocity $w'$ varies as $Ra^{3/7}$. Though the experimental results are very convincing, there may be some discussion as to the validity of some of the theoretical assumptions made by these authors. However, using the relationship that $Nu \sim Re^{2/3}$, in equation (28), leads to a power law

$$Nu \sim (Id^3)^{1/3}.$$

Our experimental results (Fig. 5), whether presented in the viscous or inertial regimes, show variations far stronger than these. Though we are not quite certain that the results will continue with the same variation asymptotically, we feel quite sure that such a transposition of classical Rayleigh–Bénard laws to the electroconvective case is not realistic. This would suggest that the flow structure in the EHD case is quite different from that with only buoyancy forces, and that any analogies made between Rayleigh–Bénard and electroconvection be done so carefully.

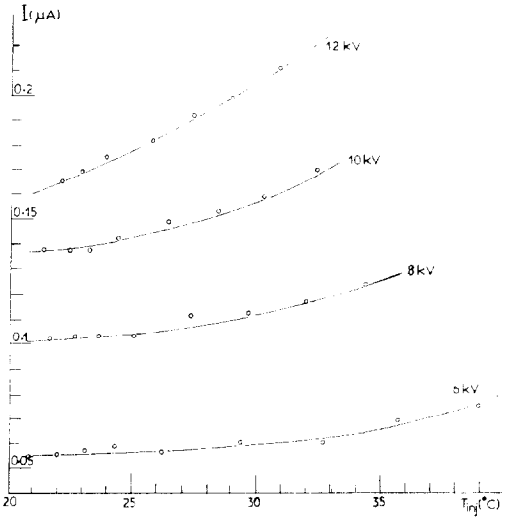


FIG. 7. The total current passing through the cell at different heat fluxes and for different voltages as a function of the temperature of the injection plate. (Case of heating and injection from the same plate.)

Finally, we note that Lazarenko *et al.* [10] attempted a somewhat general analysis of the effects of electrical forces on heat transfer and eventually reached a dependence of $Nu$ on the parameter $(Id^3)$ for both 'laminar' and turbulent flow, with upper and lower limits for the power law exponents of 0.25 and 0.5, respectively. Though our viscous regime analysis does not lead to the same parameter (ours includes a voltage dependence), it leaves little doubt as to that for the fully turbulent regime.

## 6. DISCUSSION AND CONCLUSION

Attempting to examine the results series by series did not lead us to conclude anything more definite concerning the possible power law variations, and this was compounded with the difficulty of fixing the injection level with any great precision. Figure 7 shows the total current passing through the cell for given values of the voltage as a function of the temperature of the injecting electrode. The current clearly rises somewhat dramatically with temperature for the higher voltages (+30%). The problem with this is that we have no way of knowing whether this increase in current is due to higher injection by the hot electrode or to an increase in the level of conductivity of

the liquid. Such imprecisions are unavoidable. However, we may conclude on a certain number of points:

(1) Electroconvection, in the range of parameters chosen here, appears, to first approximation, unaffected by temperature gradients and buoyancy forces.

(2) Nusselt numbers were shown to increase by up to an order of magnitude when electroconvective motion was present.

(3) In electroconvective heat transfer the flow structure appears to be different to that of natural convection.

(4) Relevant parameters governing the electrical forces were shown to be $(IVd^3)$ for viscous dominated flow and $(Id^3)$ for inertially dominated flow.

It is quite clear from this that classical heat transfer results cannot be simply transposed to the electrical case and that an analysis of electroconvective flow is needed as well as, experimentally, measurement of the velocity between the plates.

*Acknowledgements*—This work was carried out with financial support from an EEC grant (stimulation action) No. ST 2J-0151-2F. Partial support was also provided by the C.N.R.S. (action incitative Europe No. 975041). The authors would also like to express their gratitude to Mr J. L. Bély for his technical assistance, and to Drs B. Malraison and A. Castellanos for their many helpful suggestions and comments.

## REFERENCES

1. H. Senftleben and W. Braun, Der Einfluss elektrischer Felder auf den Wärmestrom in Gasen, *Z. Phys.* **102,** 480–500 (1936).
2. G. Ahsmann and R. Kronig, The influence of electric fields on the convective heat transfer in liquids, *Appl. Scient. Res.* **A2,** 235–244 (1950).
3. T. B. Jones, Electrohydrodynamically enhanced heat transfer in liquids—a review, *Adv. Heat Transfer* **14,** 107–148 (1978).
4. S. D. Savkar, Dielectrophoretic effects in laminar forced convection between two parallel plates, *Physics Fluids* **14,** 2670–2679 (1971).
5. R. Schnurmann and M. G. C. Lardge, Enhanced heat flux in non-uniform electric fields, *Proc. R. Soc. London* **A334,** 71–82 (1973).
6. E. Bonjour, J. Verdier and L. Weil, Electroconvection effects on heat transfer, *Chem. Engng Prog.* **58,** 63–66 (1962).
7. M. Takashima and K. D. Aldridge, The stability of a horizontal layer of dielectric fluid under the simultaneous action of a vertical d.c. electric field and a vertical temperature gradient, *Q. J. Appl. Math.* **29,** 71–87 (1976).
8. M. J. Gross and J. E. Porter, Electrically induced convection in dielectric liquids, *Nature (London)* **212,** 1343–1345 (1966).
9. R. J. Turnbull, Free convection from a heated vertical plate in a direct-current electric field, *Physics Fluids* **12,** 2255–2263 (1969).
10. B. R. Lazarenko, F. P. Grosu and M. K. Bologa, Convective heat transfer enhancement by electric fields, *Int. J. Heat Mass Transfer* **18,** 1433–1441 (1975).
11. J. F. Hoburg and J. R. Melcher, Internal electrohydrodynamic instability and mixing of fluids with orthogonal field and conductivity gradients, *J. Fluid Mech.* **73,** 333–351 (1976).
12. J. F. Hoburg and J. R. Melcher, Electrohydrodynamic mixing and instability induced by colinear fields and conductivity gradients, *Physics Fluids* **20,** 903–911 (1977).
13. J. F. Hoburg, Internal electrohydrodynamic instability of liquids with colinear field and conductivity gradients, *J. Fluid Mech.* **84,** 291–303 (1978).
14. N. Félici, D.C. conduction in dielectric liquids. Part I: A survey of recent progress, *Direct Current* **2,** 90–99 (1971).
15. M. E. Franke, Effect of vortices induced by corona discharge on free convection heat transfer from a vertical plate, *Trans. ASME J. Heat Transfer* **91,** 427–433 (1969).
16. J. L. Fernandez and R. Poulter, Radial mass flow in electrohydrodynamically-enhanced forced heat transfer in tubes, *Int. J. Heat Mass Transfer* **30,** 2125–2136 (1987).
17. T. Mizushina, F. Ogino, T. Matsumoto, M. Yokoyama and N. Kitano, Effect of radial electrical field on heat and momentum transfers in dielectric organic liquid for laminar flow through concentric annuli, *Int. J. Heat Mass Transfer* **23,** 1105–1115 (1980).
18. J. F. Hoburg, Temperature-gradient driven electrohydrodynamic instability with unipolar injection in air, *J. Fluid Mech.* **132,** 231–245 (1983).
19. R. F. Bradley and J. F. Hoburg, Electrohydrodynamic augmentation of forced convection heat transfer, *I.E.E.E. Trans. Ind. Applic.* **IA-21**(6), 1373–1376 (1985).
20. M. K. Bologa, V. V. Pushkov and A. B. Berkov, Electric field induced heat transfer enhancement in a gas–solid suspension heat exchanger, *Int. J. Heat Mass Transfer* **28,** 1245–1255 (1985).
21. P. Atten, F. M. J. McCluskey and A. C. Lahjomri, The electrohydrodynamic origin of turbulence in electrostatic precipitators, *I.E.E.E. Trans. Ind. Applic.* **IA-23,** 705–711 (1987).
22. A. Denat, B. Gosse and J. P. Gosse, Ion injections in hydrocarbons, *J. Electrostatics* **7,** 205–225 (1979).
23. J. Filippini, J. P. Gosse, J.-C. Lacroix et R. Tobazéon, Mise en oeuvre et application de la strioscopie à l'étude des phénomènes électrohydrodynamiques dans les liquides diélectriques, *C.R.A.S.P.* **269,** 167–170 (1969).
24. E. J. Hopfinger and J. P. Gosse, Charge transport by self-generated turbulence in insulating liquids submitted to unipolar injection, *Physics Fluids* **14,** 1671–1682 (1971).
25. J. M. Schneider, P. K. Watson and H. R. Till, Electrohydrodynamic stability of space charge limited currents in dielectric liquids, *Physics Fluids* **13,** 1948–1961 (1970).
26. P. Atten et R. Moreau, Stabilité électrohydrodynamique des liquides isolants soumis à une injection unipolaire, *J. Méc.* **11,** 471–520 (1972).
27. P. Atten, Stabilité électrohydrodynamique des liquides de faible conductivité, *J. Méc.* **14,** 461–495 (1975).
28. J. C. Lacroix, Instabilités hydrodynamiques et électroconvection lors d'injection d'ions dans les liquides isolants isotropes, State Thesis, Grenoble, France (1976).
29. J. C. Lacroix, P. Atten and E. J. Hopfinger, Electroconvection in a dielectric liquid layer subjected to unipolar injection, *J. Fluid Mech.* **69,** 539–563 (1975).
30. H. Bénard, Les tourbillons cellulaires dans une nappe, *Rev. Gén. Sci. Pures Appliquées* **11,** 1261–1271; 1309–1328 (1900).
31. Lord Rayleigh, On convective currents in a horizontal layer of fluid when the higher temperature is on the underside, *Phil. Mag.* **32,** 529–546 (1916).
32. P. Atten and J. C. Lacroix, Electrohydrodynamic stability of liquids subjected to unipolar injection: non-linear phenomena, *J. Electrostatics* **5,** 439–452 (1978).
33. N. Félici, Phénomènes hydro- et aérodynamiques dans la conduction des diélectriques fluides, *Rev. Gén. Elec.* **7**(8), 717–734 (1969).
34. T. Y. Chu and R. J. Goldstein, Turbulent convection in

a horizontal layer of water, *J. Fluid Mech.* **60**, 141–159 (1973).
35. J. W. Deardorff and G. E. Willis, Investigation of turbulent thermal convection between horizontal plates, *J. Fluid Mech.* **28**, 675–704 (1967).
36. N. Tamai and T. Asaeda, Thermal convection for large water depth and large Rayleigh numbers, *J. Hydrosci. Hydraulic Engng* **1**, 37–51 (1983).
37. N. Tamai and T. Asaeda, Sheetlike plumes near a heated bottom plate at large Rayleigh number, *J. Geophys. Res.* **89**, 727–734 (1984).
38. R. Krishnamurti, Finite amplitude convection with changing mean temperature: I—Theory; II—An experimental test of the theory, *J. Fluid Mech.* **33**, 445–463 (1968).
39. R. Krishnamurti, On the transition to turbulent convection: I—The transition from two to three dimensional flow; II—The transition to time-dependent flow, *J. Fluid Mech.* **42**, 295–320 (1970).
40. R. Krishnamurti, Some further studies on the transition to turbulent convection, *J. Fluid Mech.* **60**, 285–303 (1973).
41. L. N. Howard, Convection at high Rayleigh number, *Proc. 11th Int. Congress Appl. Mech.* (Edited by H. Görtler), pp. 1109–1115. Springer, Berlin (1966).
42. R. H. Kraichnan, Turbulent thermal convection at arbitrary Prandtl number, *Physics Fluids* **5**, 1374–1389 (1962).
43. A. Denat, B. Gosse and J.-P. Gosse, High field DC and AC conductivity of electrolyte solutions in hydrocarbons, *J. Electrostatics* **11**, 179–194 (1982).
44. W. J. Worraker and A. T. Richardson, A non-linear electrohydrodynamic stability analysis of a thermally stabilised plane layer of dielectric liquid, *J. Fluid Mech.* **109**, 217–237 (1981).
45. A. Denat, Etude de la conduction électrique dans les solvants non polaires, State Thesis, Grenoble, France (1982).
46. S. Chandrasekhar, *Hydrodynamic and Hydromagnetic Stability*. Oxford University Press, Oxford (1966).
47. J. R. Herring, Investigation of problems in thermal convection, *J. Atmos. Sci.* **20**, 325–338 (1963).
48. N. Félici, Phénomènes Hydro et Aérodynamiques dans la conduction des diélectriques fluides, *Rev. Gén. Elec.* **78**(7/8), 717–734 (1969).
49. B. Castaing, G. Gunaratne, F. Heslot, L. Kadanoff, A. Libchaber, S. Thomae, X. Z. Wu, S. Zaleski and G. Zanetti, Scaling of hard thermal turbulence in Rayleigh-Bénard convection, *J. Fluid Mech.* **204**, 1–30 (1989).

## APPENDIX A

The measured electric current in our experiments is due to two distinguishable processes: residual conduction and the migration of the injected ions (unipolar injection only). We explain briefly here how we extract the injected current ($I_{inj}$) from the measured value ($I$) (see ref. [45]).

The electrical current density, $J$, through the cell is

$$J = eE(P_i K_i + pK_p + nK_n) \tag{A1}$$

where $e$ is the unit charge; $P_i$, the concentration of injected ions per unit volume; $p$, the number of dissociated positive ions; $n$, the number of dissociated negative ions and $K_i$, $K_p$ and $K_n$ their respective mobilities. We may also write $J = J_i + J_c$, the injection plus the conduction current densities.

The one-dimensional Poisson's equation is

$$\frac{dE}{dx} = (P_i + p - n)\frac{e}{\varepsilon} \tag{A2}$$

(the total charge density is $(P_i + p - n)\cdot e$). The conservation equations of each species are

$$\frac{d}{dx}(pK_pE) = k_D\zeta - k_R pn \tag{A3}$$

$$-\frac{d}{dx}(nK_nE) = k_D\zeta - k_R pn \tag{A4}$$

where $k_D$ is the dissociation constant; $\zeta$ the molecular density of the dissociable species, and $k_R$ the recombination constant. In thermodynamic equilibrium, this is

$$k_D\zeta = k_R p_0 n_0 \tag{A5}$$

with $p_0$ and $n_0$ being the equilibrium concentrations of the positive and negative ions, respectively. Denat [45] numerically solved this set of equations with the following boundary conditions:

$$\begin{aligned} eP_i|_{x=0} &= q \\ p|_{x=0} &= 0 \\ n|_{x=d} &= 0 \\ \int_0^d E\,dx &= V. \end{aligned} \tag{A6}$$

The injecting electrode at $x = 0$ is considered positive with the collector at $x = d$ being of negative polarity. The results give the non-dimensionalized injection current density $j_i = J_i/J_{SCL}$, where $J_{SCL}\,(= \frac{9}{8}\varepsilon KV^2/d^3)$ is the current density in space charge limited injection conditions (i.e. infinite space charge density on the injector), and the non-dimensional conduction current density $j_c = J_c/J_{SCL}$ as functions of the parameters $C_i\,(= q_i d^2/\varepsilon V)$, the injection level, and $C_0\,(= \sigma d^2/2\varepsilon KV)$. $C_0$ is the conduction to injection current ratio. The value $C_0 = 1$ is reached at the saturation voltage. If $C_0 < \frac{1}{2}$ the conduction current is negligible and we take the measured current as being due to injection only. The injection level $C_i$ is then obtained using the equation $j_i = C_i\varepsilon KV^2/d^3$.

If $C_i > \frac{1}{2}$, we proceed in the following way. First, we measure the liquid conductivity $\sigma$ and deduce the value of $C_0$. From Denat's non-dimensional curves we take the corresponding value of $j_c$. By subtracting this from the total non-dimensional current, we obtain $j_i$. With these values of $j_i$ and $C_0$, the same set of curves provide $C_i$ (and, clearly, $q_i$). A further correction was carried out to take account of field enhanced conduction, again using the results by Denat [45]. Briefly, we consider that the saturation current is increased by a numerical factor, varying between 1.5 and 4.5 in our experimental conditions, depending on the field $E$, the permittivity $\varepsilon$. Although Denat's calculations are valid under hydrostatic conditions, they are a good approximation in our case. This is due to the fact that for weak injection, liquid motion has little influence on charge transfer since the current is limited by the rate at which the ions are produced at the electrode and this is independent of the dynamical state of the system. Then, the transported charge is almost the same with or without liquid motion.

## APPENDIX B

The lower plate is heated from time $t = 0$ and the heat is then transferred by the liquid and by the Plexiglas frame to the upper plate which is kept at constant temperature. For each medium (liquid, copper, Plexiglas) the heat equation is

$$\rho C_p\left(\frac{\delta T}{\delta \tau}\right) + \nabla H = 0. \tag{B1}$$

We assume for simplicity that the temperature gradients in the liquid and in the Plexiglas are vertical only and that the copper plate is isothermal. Integrating equation (B1) over the depth of the copper plate, i.e. from $z = 0$ to $d_1$, we obtain

$$H_1 = H_0 - \rho_c C_{pc} d_1 \frac{\delta T_1}{\delta t} \tag{B2}$$

where $H_0$ is the heat flux furnished to the plate and $H_1$ is that passing from the plate to the liquid and Plexiglas. The subscript C refers to copper. If we now integrate the heat equation over each medium between the two electrode plates ($d_1 \leqslant z \leqslant d_2$) we obtain for the liquid and for the Plexiglas, respectively

$$\rho_L C_{pL} \int_\Omega \frac{\delta T}{\delta t} dx\, dy\, dz + (H_{L2} - H_{L1}) S_L = 0 \qquad (B3)$$

$$\rho_P C_{pP} \int_{\Omega'} \frac{\delta T}{\delta t} dx\, dy\, dz + (H_{P2} - H_{P1}) S_P = 0. \qquad (B4)$$

(Subscripts 1 and 2 refer to the lower and upper plates, respectively.)

For the first terms in equations (B3) and (B4) we will use the approximation that they can be represented as mean values over the whole volume $\Omega$

$$\rho C_p \int_\Omega \frac{\delta T}{\delta t} dx\, dy\, dz = \frac{1}{2} m C_p \frac{\delta (T_1 + T_2)}{\delta t} \qquad (B5)$$

($m$ is the mass of the medium in question). Using equation (B5), the addition of equations (B3) and (B4) gives

$$\frac{1}{2}(C_{pL} m_L + C_{pP} m_P) \frac{\delta (T_1 + T_2)}{\delta t} + S_L H_{L2} + S_P H_{P2} - S_L H_{L1} - S_P H_{P1} = 0 \qquad (B6)$$

where

$$(S_L H_{L1} + S_P H_{P1}) = S_C H_1 = S_C H_0 - m_C C_{pC} \frac{\delta T_1}{\delta t}. \qquad (B7)$$

(See equation (B2).) We now make the usual approximation that the flux at the upper plate (at constant temperature) is equal to the product of the thermal conductivity and an average temperature gradient. With $T_2$ fixed, we have

$$\frac{\delta T_1}{\delta t} = \frac{\delta (T_1 + T_2)}{\delta t} = \frac{\delta (T_1 - T_2)}{\delta t}$$

and equation (B6) becomes

$$\frac{1}{2}(C_{pL} m_L + C_{pP} m_P) \frac{\delta (T_1 - T_2)}{\delta t} + S_L \kappa_L \frac{(T_2 - T_1)}{(d_2 - d_1)} + a S_P \kappa_P \frac{(T_2 - T_1)}{(d_2 - d_1)} - S_C H_0 + m_C C_{pC} \frac{\delta (T_1 - T_2)}{\delta t} = 0. \qquad (B8)$$

This equation has a simple analytic solution

$$T_1(t) - T_2 = (T_1(0) - T_2) \exp\left(\frac{-t}{\tau}\right) + \frac{Q(d_2 - d_1)}{S_L \kappa_L + a S_P \kappa_P} \left(1 - \exp\left(\frac{-t}{\tau}\right)\right) \qquad (B9)$$

where

$$Q = S_C H_0 \qquad (B10)$$

and

$$\tau = \left(\frac{1}{2} C_{pL} m_L + \frac{1}{2} C_{pP} m_P + C_{pC} m_C\right) \frac{(d_2 - d_1)}{S_L \kappa_L + a S_P \kappa_P}. \qquad (B11)$$

Equations (B9) and (B11) are equations (13) and (14) given in the main text. Since the $\Delta T(t)$ variation is exponential then we can conclude that the 'thermal resistance' of the liquid is independent of $T$ in our conditions.

Let us note that we implicitly assumed that the conduction in the Plexiglas in the transitory regime was analogous to that in the steady-state regime. We verified this for very weak perturbations of the equilibrium state. By recording the variation of $\Delta T$ in the hydrostatic case (heating from above) we saw that the relaxation was of the exponential type (see equation (B9)) and that the time constant obtained was $\tau_0 = 44.8$ min. This value introduced into equation (B11) gives once again a value for $a$ of 0.27.

## AUGMENTATION DU TRANSFERT THERMIQUE A TRAVERS UNE COUCHE HORIZONTALE DE LIQUIDE DU A L'ELECTROCONVECTION ENTRE DEUX PLAQUES PLANES ET PARALLELES

**Résumé**—On présente une étude du transfert thermique à travers une couche horizontale de liquid dû à l'électroconvection entre deux plaques planes et parallèles. Une injection unipolaire d'ions peut être créée soit à l'électrode supérieure soit à l'électrode inférieure, la couche étant chauffée indépendamment en haut ou en bas. Ces quatre situations sont examinées. En régime transitoire, il est possible de calculer le nombre de Nusselt en s'appuyant sur un modèle électrique simple (circuit Résistance–Capacité en parallèle). Les valeurs obtenues peuvent augmenter d'un ordre de grandeur en présence de champ électrique par rapport au cas purement thermique et sont en bon accord avec les résultats en régime stationnaire. Dans tous les cas considérés, les forces de gravité sont négligeables par rapport à la force de Coulomb. A l'aide d'une analyse de l'état stationnaire, on déduit les paramètres gouvernant le transfert thermique; les produits $IVd^3$ en régime non-turbulent, et $Id^3$ en régime turbulent.

## VERBESSERUNG DES WÄRMEÜBERGANGS DURCH ELEKTROKONVEKTION AUFGRUND DER INJEKTION EINER RAUMLADUNG ZWISCHEN ZWEI PARALLELE PLATTEN

**Zusammenfassung**—Der Wärmeübergang zwischen zwei parallelen Platten bei Elektrokonvektion wird untersucht. Ein unipolarer Ionenstrom kann entweder an der oberen oder an der unteren Elektrode eingebracht werden, wobei gleichzeitig die Flüssigkeitsschicht von oben oder unten geheizt wird (stabile oder instabile Schichtung). Diese vier unterschiedlichen Konfigurationen werden getrennt behandelt. Das Übergangsgebiet wird analytisch untersucht. Unter Verwendung einer Analogie zwischen dem Experiment und einem elektrisch parallel geschalteten Widerstands-Kapazitäten-Modell wird damit die Berechnung der thermischen Nusselt-Zahl möglich. Die so ermittelten Näherungswerte zeigen eine Zunahme der Nusselt-Zahl um bis zu einer Größenordnung und stimmen sehr gut mit stationären Daten überein. Auf diese Weise wird demonstriert, daß für alle betrachteten Fälle die elektrischen Einflüsse vollkommen über die Auftriebseffekte dominieren. Eine kurze Analyse des stationären Zustandes liefert die für den Wärmeübergang wesentlichen Parameter: $Id^3$ für die vollständig turbulente Strömung und $IVd^3$ für nicht-turbulente Bedingungen.

# ИНТЕНСИФИКАЦИЯ ТЕПЛОПЕРЕНОСА ЗА СЧЕТ ЭЛЕКТРОКОНВЕКЦИИ, ИНДУЦИРОВАННОЙ ПРОСТРАНСТВЕННЫМ ЗАРЯДОМ МЕЖДУ ПАРАЛЛЕЛЬНЫМИ ПЛАСТИНАМИ

**Аннотация**—Исследуется теплоперенос между двумя параллельными пластинами за счет электроконвекции. Ввод ионов одного знака может осуществляться либо у верхнего, либо у нижнего электрода, а нагрев слоя жидкости—сверху или снизу (при устойчивой или неустойчивой стратификации). Отдельно рассматриваются эти четыре возможных конфигурации. Проводится анализ для случая нестационарного режима, позволяющий рассчитать тепловое число Нуссельта с учетом аналогии с электрической цепью сопротивлений и конденсаторов с параллельным соединением. Аппроксимированные таким образом значения показывают увеличение числа Нуссельта на порядок и очень хорошо согласуются с данными для стационарного случая. Показано, что во всех рассматриваемых случаях электрические эффекты преобладают над эффектами подъемных сил. На основе краткого анализа стационарного состояния получены соответствующие определяющие параметры теплопереноса для полностью турбулентного течения и в условиях отсутствия турбулентности.